Soft x-ray resonant magnetic scattering investigation of stable magnetic configurations in patterned rings

F. Y. Ogrin,[1,a)] E. Sirotkin,[1] G. van der Laan,[2,3] G. Beutier,[3] C. A. Ross,[4] W. Jung,[4] and R. Menon[5]
[1]*School of Physics, University of Exeter, Exeter, EX4 4QL United Kingdom*
[2]*STFC Daresbury Laboratory, Warrington, WA4 4AD United Kingdom*
[3]*Diamond Light Source, Didcot, Oxfordshire, OX11 0DE United Kingdom*
[4]*Department of Materials Science and Engineering, MIT, Cambridge, Massachusetts, MA 02139 USA*
[5]*Research Laboratory of Electronics, MIT, Cambridge, Massachusetts, MA 02139 USA*

(Presented on 8 November 2007; received 11 September 2007; accepted 19 October 2007; published online 6 February 2008)

The first experimental results of soft x-ray resonant magnetic scattering from a pattern of microscopic Permalloy rings are reported. Experimental measurements and simulations of the scattering from the stable magnetic configurations such as "vortex" and "onion" commonly observed for the ring structures are presented. Variations in the diffraction profile as a function of field are discussed in the context of the simulation results, which show a good agreement with the behavior of the experimental data. © *2008 American Institute of Physics*.
[DOI: 10.1063/1.2831392]

INTRODUCTION

In studying magnetic nanostructures, neutron and x-ray radiation offer a great advantage due to the ability to probe the material with high resolution and without affecting the magnetic state of the sample. Typically, polarized neutron reflectivity, small angle neutron scattering, and soft x-ray resonant magnetic scattering (SXRMS) have been used to investigate the in-depth magnetic profile of nanostructures which can be adapted due to artificially imposed structures (such as in multilayer films[1,2]) or due to induced interactions between the local magnetic moments.[3,4] In recent years, however, the focus of application has been shifting to the lateral variation of the magnetization,[5–8] putting emphasis on the magnetic correlation in the surface plane of the film. This is of particular interest because many technological devices, such as storage media or magnetoresistive random access memory, are based on laterally patterned materials. The ability to characterize the averaged magnetic properties of the nanostructures becomes henceforth a valuable asset. In this paper, we report on SXRMS from patterned micron-size magnetic rings, and demonstrate the capacity of this technique to identify complex two-dimensional (2D) magnetic configurations such as "vortex" and "onion" states.

SXRMS utilizes the diffraction properties of polarized photons to probe the moments of the resonantly excited elements in the material.[9] Strong resonant enhancement of the magnetic scattering is achieved by tuning the photon energy to an appropriate absorption edge, making the technique element and shell sensitive. For $3d$ transition metals, the excitation of a $2p$ core electron into the unoccupied $3d$ states ($L_{2,3}$ absorption edges) leads to a strong resonance enhancement in the soft x-ray energy region.[10] Both the in-depth and lateral distribution of the magnetization can be probed on a length scale down to the photon wavelength, i.e., ~ 1 nm, which makes it well suited for dimensions currently pursued in storage media applications. A big advantage over neutrons is that soft x rays are confined to a narrow beam with a high transverse coherence (up to 50 μm in the case of third generation synchrotron radiation facilities[11]). Therefore, the in-plane distribution of the magnetic moments can be studied on length scales relevant to ferromagnetic domains and patterned nanostructures. So far, the application of SXRMS has included characterization of structural and magnetic properties of layered and domain systems.[3,5,7,9,12–15] Application to patterned materials, however, has hardly been undertaken. In one particular study, Chesnel *et al.*[16] applied the technique to a patterned periodic structure of Co/Pt nanolines and evidenced the additional Bragg scattering due to the antiferromagnetic arrangement of the magnetic domains in the demagnetized state and at the coercive point of the hysteresis curve.

Here, we present, to our knowledge, the first SXRMS experiments on 2D patterned magnetic arrays and explore the possibility of using this technique to determine the magnetic configurations in lateral magnetic nanostructures. As object of study, we have chosen a pattern of *microscopic* rings. Ring structures have recently attracted much attention because of the existence of flux-closed magnetic configurations, i.e., vortex states (see inset in Fig. 1).[17] These are particularly interesting for diffraction experiments because the vortex configuration has a well-defined magnetic structure that can be easily modeled and examined by means of simulation. This is also true for the onion state, which is also a stable state of the magnetic configuration formed at remanence (inset in Fig. 1). The main objective of our study was to explore the soft x-ray scattering profiles from the predicted vortex and onion states and to compare these with the simulated curves of the ideal configurations. In order to provide a well-defined structure of the magnetic configuration, the dimensions of rings were chosen in the region of $1-10$ μm scale. This length scale is also optimal for fabrication of patterned arrays on a sufficiently large area, which

[a)]Electronic mail: f.y.ogrin@exeter.ac.uk.

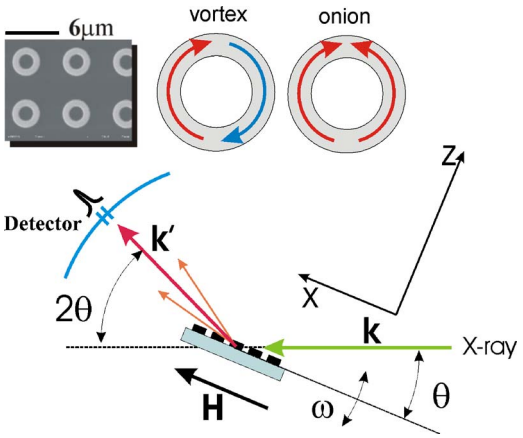

FIG. 1. (Color online) Schematic diagram of the experimental scattering geometry. The insets show, from left to right, a scanning electron microscopy (SEM) image for a small section of the sample (Ref. 8) and the schematic representations of the vortex and onion states, where the red and blue arrows indicate the ideal orientations of the magnetization in the rings.

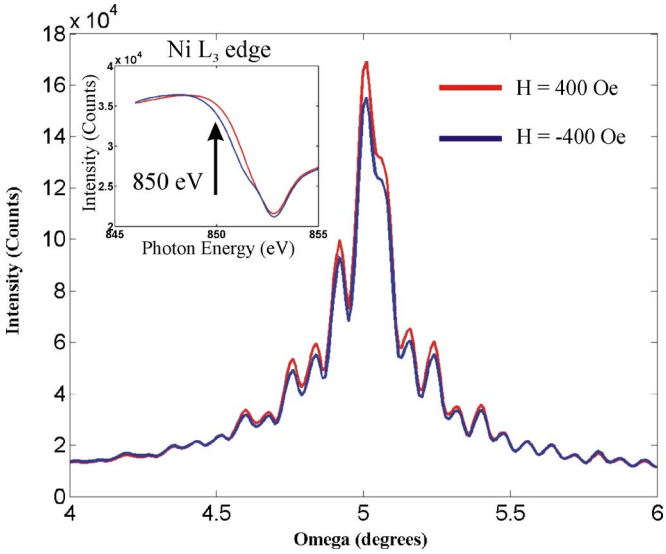

FIG. 2. (Color online) Reflectivity rocking curves around $\omega=5°$ ($2\theta=10°$) for opposite fields (blue and red) with the photon energy fixed to 850.7 eV. Inset: reflectivity as a function of photon energy across the Ni L_3 edge for opposite magnetic fields, +400 and −400 Oe (blue and red). The difference between the curves corresponds to the scattering arising from the magnetic structure.

are normally needed for measurements with x ray and neutron scattering.

EXPERIMENTAL

Samples were fabricated using zone plate array lithography,[18] combined with the lift-off process. Each sample contained three patches of 2.5×5 mm^2 of patterned rings, which were closely "stitched" with a gap of ~50 μm. Rings had dimensions of 3.2 μm in outer diameter and 700 nm in width, and formed a periodic square array with 5.6 μm of center-to-center separation. The magnetic layer was made of Permalloy, Ni80Fe20, with the average thickness of ~25 nm.

Experiments were carried out on the soft x-ray undulator beamline 5U.1 of the Synchrotron Radiation Source (SRS) at Daresbury Laboratory, UK. All diffraction measurements were performed using left-circularly polarized x rays in reflection geometry in a high-vacuum diffractometer.[19] The magnetic field was applied in the longitudinal direction, i.e., along the intersection of the sample surface and scattering plane (see Fig. 1). The photon energy was tuned at the Ni L_3 absorption edge, to the position of maximum magnetic scattering dichroism for opposed field orientations (see inset in Fig. 2). The scattered intensity was measured using a "point detector" (a photosensitive diode behind a 0.3 mm slit), fixed at an angle 2θ to the incident beam, and "rocking curves" were recorded by varying the sample angle ω around θ.

DISCUSSION

The intensity I measured at a vector position $\mathbf{q}$ in reciprocal space is the square modulus of the sum of the charge scattering amplitude $A_c(\mathbf{q})$ and the magnetic scattering amplitude $A_m(\mathbf{q})$, i.e., $I(\mathbf{q})=|A_c(\mathbf{q})+A_m(\mathbf{q})|^2$. In our sample, the magnetic configuration has the same periodicity as the patterned array, so that charge and magnetic scattering coincide in reciprocal space. Since the amplitude of the magnetic scattering is several orders of magnitude lower than that of the charge scattering, the pure magnetic contribution to the intensity $|A_m(\mathbf{q})|^2$ is small compared to the interference term $2\mathrm{Re}[A_c(\mathbf{q})A_m(\mathbf{q})]$ and only the latter is taken into account. Thus, the measured intensity appears as a linear function of the Fourier transform of the magnetization, projected along a vector determined by the x-ray polarization and reflection angle θ. Further details of the formalism can be found in Ref. 20. By subtracting two spectra taken under identical conditions, except for an applied magnetic field, the charge contribution can be eliminated, and the remaining interference term contains the magnetic contribution.

Figure 2 shows the diffraction profile obtained for a ω-scan at an incident angle of $\theta=5°$ in a saturating magnetic field of 400 Oe applied in the two opposite directions. The main contribution to the intensity comes from the charge scattering, while the difference between both curves comes from the interference term. In order to isolate this magnetic contribution in the total intensity, one has to subtract the contribution from the charge scattering. In our analysis we have done this by subtracting the diffraction profile obtained at the saturated state from each pattern obtained at other values of the applied field. To investigate this further, we have simulated the scattering profile from a pattern of rings having three distinctive states: onion, vortex, and "reversed onion" (where the average moment is opposite to the field direction). In our model, we used 200×200 cell vector maps, each vector representing the magnetization of a square patch of 140×140 nm^2. Each of the states (or configurations) has been formed by orienting the vectors as in the ideal pattern. For instance, in the case of the vortex, all vectors were circumferentially oriented, as schematically shown in the inset in Fig. 1. The 2D-SXRMS response function has been numerically calculated using the solution given in Ref. 20. The output of the model produces an intensity function $I(\mathbf{q})$ in 2D reciprocal space (q_x,q_y), in which one coordinate is fixed $(q_y=0)$ and the intensity variation is extracted only for the q_x component. Figure 3 displays the three resulting solutions. We show the experimental profiles obtained for the

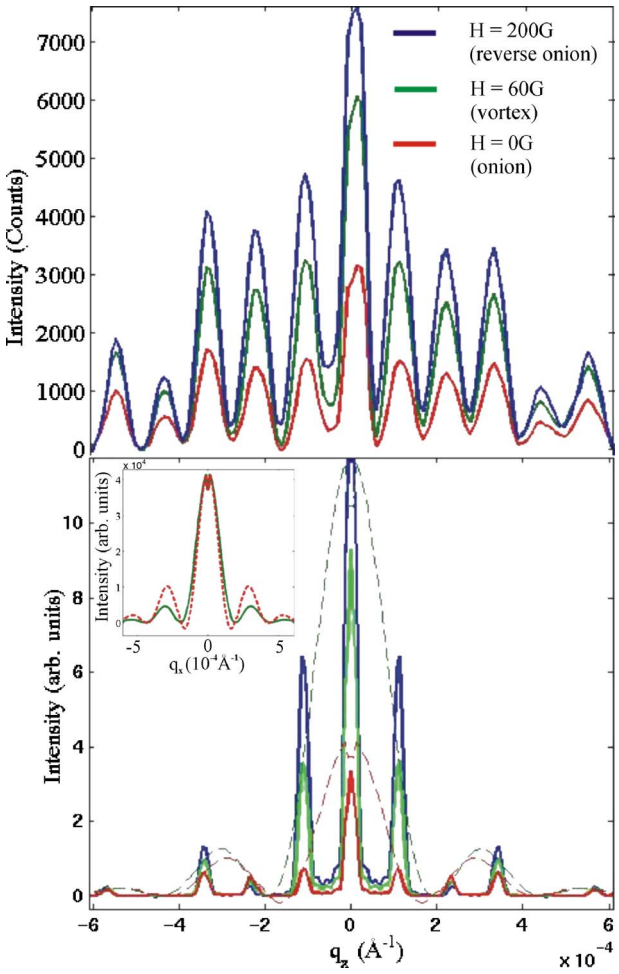

FIG. 3. (Color online) Top panel: magnetic diffraction profiles measured for three different values of the applied field [0.0 Oe (red), 60 Oe (green), and 200 Oe (blue)] after saturating the sample at −400 Oe. The applied fields correspond to the expected configurations of the onion, vortex, and reverse onion states, respectively (according to the AGM measurements). Bottom panel: magnetic diffraction profiles simulated for the same "ideal" configurations. In order to extract the magnetic contribution each curve corresponds to the difference between the profiles measured at the specified field value and the profile measured the saturation field (−400 Oe). The dashed lines show the corresponding diffraction profile for vortex (green) and onion (red) from the magnetic configuration of a single ring (the form factor). The inset shows the same, but normalized form factors to demonstrate the amount of the profile variation.

different fields (0, 60, and 200 Oe), where we expect to find the different configurations (onion, vortex, and reversed onion, respectively).

Although the profiles do not give a precise match, the characteristics of the simulated curves exhibit very similar trends as those obtained experimentally. The overall intensity (subtracted by the saturated value) is increasing steadily as the field is increased from negative to positive saturation. This is because the intensity of the magnetic contribution to the scattering scales linearly with the magnetization component parallel to the outgoing wave vector. However, one can also perceive that the peak profile changes at different points of the hysteresis loop, e.g., the relative height of the peaks is different for the onion and vortex states. This difference is especially notable in the simulated profile (Fig. 3). It is seen that in this case the intensity of the first-order peak is greatly reduced. The change in the peak profile is, as we might expect, directly related to the change in the magnetic configuration as the field is traversing through the remanent state, and then further to positive field corresponding to the stage of formation of the onion, vortex, and reversed onion states.

The simulated results show that the intensity variation of the first-order (or third-order) peaks is particularly sensitive to a change in the magnetic configuration. Generally, a change in the "magnetic shape" of each element leads to a change of the "envelope" of the Bragg peaks, the so-called "form factor." As seen from Fig. 3, the intensity change is particularly large for the peaks that are at the position of the maximum variation. At the same time, the change of the magnetic shape affects the entire diffraction profile (inset in Fig. 3). In general, this can be confirmed by following the variation of each diffraction peak as a function of applied field, however, the experimental results are complicated by instrumental characteristics. The measured intensity $I(q_x)$ is not a one-dimensional cut in 2D reciprocal space but rather corresponds to the integrated intensity over the available q_y range for each q_x. The exact modeling in this case relies on the assumption of an ideal (Gaussian) shape of the beam, which is usually more complex. A further complication for this range of sample dimensions ($\sim$10 μm) arises from the limited instrumental resolution in q_y, so that the diffraction pattern is not fully resolved. One can still use modeling to take these facts into account, be it at the price of a significant increase in complexity. In general, submicron dimensions would be preferred, since it would allow us to resolve the structural information of the entire 2D reciprocal space.

We would like to acknowledge financial and technical support from the SRS facility at STFC Daresbury Laboratory, UK, and financial support from National Science Foundation, US.

[1] N. Jaouen *et al.*, Phys. Rev. B **66**, 134420 (2002).
[2] K. V. O'Donovan, J. A. Borchers, C. F. Majkrzak, O. Hellwig, and E. E. Fullerton, Phys. Rev. Lett. **88**, 067201 (2002).
[3] G. Beutier *et al.*, Phys. Rev. B **71**, 184436 (2005).
[4] S. Langridge, J. Schmalian, C. H. Marrows, D. T. Dekadjevi, and B. J. Hickey, Phys. Rev. Lett. **85**, 4964 (2000).
[5] H. A. Durr, E. Dudzik, S. S. Dhesi, J. B. Goedkoop, G. van der Laan, M. Belakhovsky *et al.*, Science **284**, 2166 (1999).
[6] C. Fermon *et al.*, Physica B **267–268**, 162 (1999).
[7] A. Haznar *et al.*, J. Synchrotron Radiat. **11**, 254 (2004).
[8] F. Y. Ogrin *et al.*, IEEE Trans. Magn. **43**, 2731 (2007).
[9] G. van der Laan, Curr. Opin. Solid State Mater. Sci. **10**, 120 (2006).
[10] G. van der Laan and B. T. Thole, Phys. Rev. B **43**, 13401 (1991).
[11] G. Beutier *et al.*, Rev. Sci. Instrum. **78**, 093901 (2007).
[12] T. P. A. Hase *et al.*, Phys. Rev. B **61**, R3792 (2000).
[13] J. F. MacKay *et al.*, Phys. Rev. Lett. **77**, 3925 (1996).
[14] R. M. Osgood *et al.*, J. Appl. Phys. **85**, 4619 (1999).
[15] J. B. Kortright *et al.*, Phys. Rev. B **64**, 092401 (2001).
[16] K. Chesnel *et al.*, Phys. Rev. B **66**, 024435 (2002).
[17] F. Castano, A. Eilez, W. Jung, C. Frandsen, and C. A. Ross, Phys. Rev. B **69**, 144421 (2004).
[18] W. Jung, F. J. Castaño, D. Morecroft, C. A. Ross, R. Menon, and H. I. Smith, J. Appl. Phys. **97**, 10K113 (2005); D. J. D. Carter, D. Gil, R. Menon, M. K. Mondol, H. I. Smith, and E. H. Anderson, J. Vac. Sci. Technol. B **17**, 3449 (1999).
[19] M. D. Roper *et al.*, Nucl. Instrum. Methods Phys. Res. A **467–468**, 1101 (2001).
[20] G. van der Laan, "Soft X-ray resonant magnetic scattering of magnetic nanostructures," C. R. Phys. (in press).